

Synthesis and Characterization of CdS Nanoparticles Grown in a Polymer Solution using in-situ Chemical Reduction Technique

Shujahadeen B. Aziz¹, Mariwan A. Rasheed², Salah R. Saeed³, Omed Gh. Abdullah^{1,*}

¹ Advanced Materials Research Lab., Department of Physics, College of Science, University of Sulaimani, 46001, Kurdistan Region, Iraq.

² Development Centre for Research and Training (DCRT), University of Human Development, Kurdistan Region, Iraq.

³ Charmo Research Center, Charmo University, Peshawa Street, Chamchamal, 46023, Sulaimani, Kurdistan Region, Iraq.

*E-mail: omed.abdullah@univsul.edu.iq

Received: 3 January 2017 / Accepted: 12 February 2017 / Published: 12 March 2017

Cadmium sulfide (CdS) nanoparticles embedded in poly(vinyl alcohol) (PVA) in the form of films with different CdS content have been prepared successfully using in-situ chemical reduction technique and casting of aqueous solutions. The nano-CdS characterised using UV-Vis spectroscopy which shows an absorption shoulder around 500 nm confirming the formation of CdS nanoparticles. Moreover, the linear increase in absorbance with increasing CdS concentration revealed that the CdS nanoparticles are homogeneously distributed in the host PVA polymer matrix. To detect structural changes, XRD and FTIR spectra of pure and CdS doped PVA films have been analysed. FTIR analysis evidently shows the interaction between CdS nanoparticles with the hydroxyl groups of PVA. It is also found that the ac conductivity of doped PVA samples increases with the increase of CdS content as well as frequency. The calculated values of frequency exponent (s) suggest that the electrical conduction is followed by the correlated barrier hopping (CBH) model. The temperature dependence of ac conductivity also indicated that the minimum activation energy associated with the maximum conductivity composition. The experimental results reveal that the optical and electrical behaviour of PVA can be improved significantly by the addition of a small amount of CdS nanoparticles. This enhanced properties of PVA/CdS nanocomposite proposed to be used in optoelectronic devices.

Keywords: polymer nanocomposites; CdS nanoparticles; conduction mechanism; ac conductivity; activation energy.

1. INTRODUCTION

Development of polymer-based nanocomposite is a fast-growing area of scientific research, owing to the excellent properties at low filler concentration [1,2]. Significant efforts are focused on the ability to prepare and control the nanoscale structures through innovative synthetic approaches.

Therefore, present studies were centred around developing simpler and inexpensive techniques to produce polymer nanostructures [3-5]. It is well quoted in the literature that the characteristics of particulate polymer nanocomposite are sensitive to the nanoparticles size [6], shape [7], and the way in which it dispersed and interacted with the host polymer matrix [8].

During the past decade, nanosize cadmium sulfide (CdS) as one of the most important II-VI group semiconductors, have attracted considerable interest in technological aspects owing to their critical applications in solar cells, light-emitting diodes LEDs, electronic, optoelectronic, and quantum size effect semiconductors devices [9-11]. Therefore, much effort has been directed to develop simpler and inexpensive techniques to produce this nanostructure [12]. Several methods have been used to synthesize CdS nanoparticles, nanowires and nanorods, such as; hydrothermal method [13], chemical bath deposition [14], in situ thermolysis method [15], ultrasound-assisted method [16], gamma radiolytic method [17], nanosecond laser irradiation assistant [18], and many other complex and simple procedures.

Poly(vinyl alcohol) (PVA) has attracted significant attention due to its superior optical and mechanical properties over a long range of temperature [19]. PVA has carbon chain backbone with hydroxyl groups (-OH) attached to methane carbons; these (-OH) groups can be a source of hydrogen bonding, and hence help the formation of inorganic nanoparticles inside the PVA material [20,21]. While, the relatively large band gap of PVA, lowers the optical absorption and light harvesting, and, therefore, limits its application as an active layer in organic solar cells [22]. Thus, controlling of the band gap is extremely important during design and synthesise new materials for organic solar cells [23]. The band gap of organic materials can be controlled by introducing inorganic nanoparticles in the polymer matrix [24,25]. As well, incorporation of just a few weight percent of the well-dispersed nanoparticles into PVA matrix has a profound impact on the structural, optical, electrical, and mechanical properties of the polymer matrix [26,27]. The outcome of this technology has attracted much attention in view of their potential applications in electrical and optical devices [8]. Detailed studies of the polymer doped with different filling levels of a particular filler allow the possibility of choice of the desired properties [28].

Keeping this in view, in order to find solid polymer nanocomposites with tuned properties for electronic and photonic applications, an attempt has been made to prepare nano-CdS dispersed in PVA polymer films with different concentrations of CdS by a simple and inexpensive chemical reduction method. Electrical properties have been studied aiming to understand the nature of the charge transport predominant within these materials, to interpret the conduction mechanism taking place in this system.

2. MATERIALS AND EXPERIMENTS

2.1 Materials

The chemical materials used in this study were cadmium nitrate ($\text{Cd}(\text{NO}_3)_2$) with a molecular weight (236.42 g/mol) supplied by Merck, and sodium sulfide nonahydrate ($\text{Na}_2\text{S}\cdot 9\text{H}_2\text{O}$) with a molecular weight (240.18 g/mol) provided by Sigma-Aldrich. Low molecular weight Poly(vinyl alcohol) (PVA) $[\text{C}_2\text{H}_4\text{O}]_n$ (98-99% hydrolyzed) provided by Alfa Aesar, used as a stabilizer and

capping of synthesised CdS nanoparticles, and distilled water used as a solvent. These materials were used without any further purification.

2.2 Preparation of nanocomposite films

An aqueous solution of pure Poly(vinyl alcohol) was prepared by dissolving 1 g of PVA in 35 mL distilled water using magnetic stirring for one hour at 90°C until a clear homogeneous solution has been formed. Different molar concentrations (0.01, 0.02, 0.03 and 0.04 M) of cadmium nitrate ($\text{Cd}(\text{NO}_3)_2$) as a source of cations (Cd^{+2}), and sodium sulfide nonahydrate ($\text{Na}_2\text{S}\cdot 9\text{H}_2\text{O}$) as a source of anions (S^{-2}) were separately prepared in the 5 mL distilled water at room temperature. The two prepared solutions were added dropwise with ratio 1:1 to the PVA solution under continuous stirring. The dissolved Cd^{+2} ions react with released S^{-2} to form nano-CdS nuclei, and the PVA solution act as a stabilizer and a capping agent to protect the produced nanoparticles from aggregation. The colorless solution of PVA changed to yellow-orange immediately by adding a few drops of nitrate solution, which consistent with the color of the cadmium sulfide (CdS). The solutions were poured into a clean plastic Petri dishes (8.2 cm in diameter), and left to dry at room temperature ($\sim 32^\circ\text{C}$) in the open air for two weeks for films to form. The dried formed films were peeled off and transferred into desiccator with blue silica gel for continues drying. The thickness of the prepared films was in the range between (25-30) μm .

2.3 Characterization techniques

Double beam UV-VIS-NIR spectrophotometer (Perkin Elmer, Lambda 25) is used to measure the absorbance of prepared pure PVA and PVA/CdS polymer nanocomposite films in the wavelength range (190-1100) nm.

The X-ray diffraction (XRD) patterns of prepared films were collected using X-ray diffractometer (X'PERT-PRO) equipped with Cu $K\alpha$ as a radiation source ($\lambda = 0.154$ nm) in the 2θ range ($10^\circ - 50^\circ$) at a scanning rate of 2°min^{-1} .

The FTIR spectra of the hybrid films were obtained by a Perkin Elmer FTIR spectrometer (Spectrum 100, Waltham, Massachusetts, USA) in the wavelength range of $4,000$ to 400 cm^{-1} .

The Precision LCR Meter (Agilent/HP 4284A) operating at a frequency range 1 KHz to 1 MHz and, temperature range ($30 - 110$) $^\circ\text{C}$ is used to measure the electrical properties. The films were sandwiched between two Aluminum electrodes (2.5 cm in diameter) under spring pressure. The K-type thermocouple (accuracy of $\pm 0.1^\circ\text{C}$) was used to measure the temperature of the sample inside the chamber.

3. RESULTS AND DISCUSSION

3.1 Optical absorbance

Optical absorption spectra of pure and doped PVA films with different concentration of CdS are shown in Fig 1. It is seen that the doping of CdS in PVA polymer matrix exhibited additional

absorption shoulder around 500 nm for the CdS particles [29], in addition to the onset absorption at 250 nm assigned to $\pi \rightarrow \pi^*$ transition of PVA materials [30,31]. The nanoparticles are known to have an absorption edge, which is shifted with respect to the bulk material towards shorter wavelengths. This blue shift is thus taken as an indication of the formation of nanoparticles and can be used to evaluate the particles size [32-34]. The absorption threshold of bulk CdS was around 515 nm [35]. Thus, the appeared peak at 500 nm is due to the small size of the dispersed nano-CdS in the PVA matrix, and its intensity is continuously increasing with increasing nano-CdS concentration [34].

The two abrupt absorption shoulders at 500 and 250 nm, known as the fundamental absorption edge, which can be used to determine the band gap of CdS nanoparticles and polymer nanocomposite respectively [36,37]. Babu *et al.* [38] have also reported the similar behaviour, for CdS nanoparticles embedded in DMF.

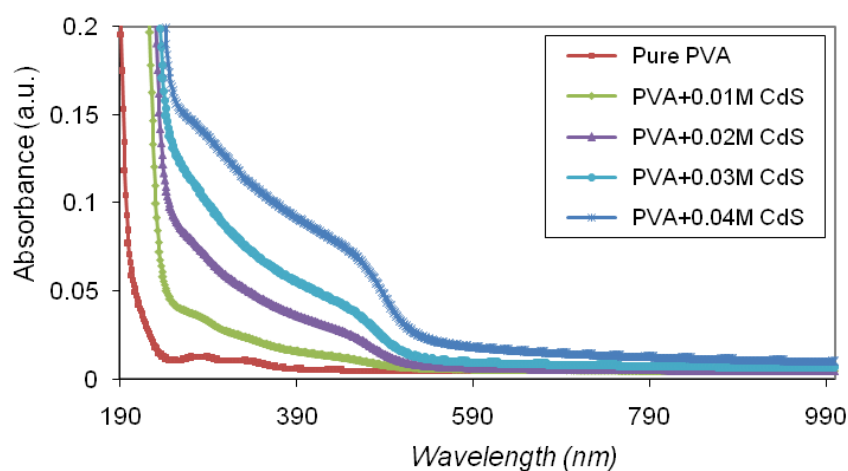


Figure 1. Absorbance spectra for pure and doped PVA with different concentration of CdS nanoparticles.

3.2 XRD analysis

X-ray diffraction (XRD) patterns of as-prepared pure and CdS dispersed PVA polymer nanocomposites observed in the present study are shown in Fig. 2. The diffraction pattern of pure PVA displays the broad peak around $2\theta \approx 19.26^\circ$ depicting the semi-crystalline nature of PVA [39,40]. This may be due to the presence of strong intra-molecular hydrogen bonding in individual monomer unit of PVA, as well as inter-molecular hydrogen bonding between its different monomer units [36]. The intensity of PVA peak in the nanocomposite sample is decreased, after embedding CdS nanoparticles. On account of CdS nanoparticles embedding, the hydrogen bonds of hydroxyl groups of the PVA chains may break, and molecular chains are free to rotate [41].

The XRD pattern of the PVA/CdS nanocomposite films (Fig. 2b,c) could not represent the characteristics peaks for CdS nanoparticle (Fig. 2d, the standard JCPDS No. 41-4019), this mainly due to the very small concentration of CdS compared with that of the host semi-crystalline PVA, therefore the amorphous contribution dominated the scattering spectrum in PVA/CdS nanocomposite films, and

hence it was not possible to clearly identify the CdS contribution in the overall scattering spectra [37]. Therefore, the salient features of the PVA/CdS nanocomposite films are characterised using the Fourier transform infrared spectrometry.

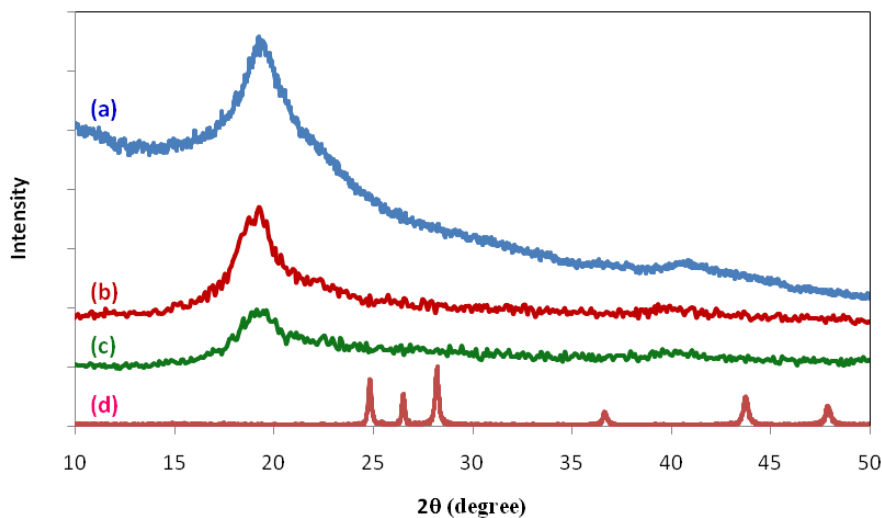


Figure 2. The X-ray diffractogram of: (a) pure PVA, (b) PVA doped 0.02M CdS (c) PVA doped 0.04M CdS, and (d) pure CdS.

3.3 FTIR analysis

The Fourier transform infrared (FTIR) spectra for the pure and different concentration of CdS doped PVA films are presented in Fig. 3. The FTIR spectrum of pure PVA film exhibits several characteristic bands of stretching and bending vibrations of C-O, C-H, C=C and O-H groups.

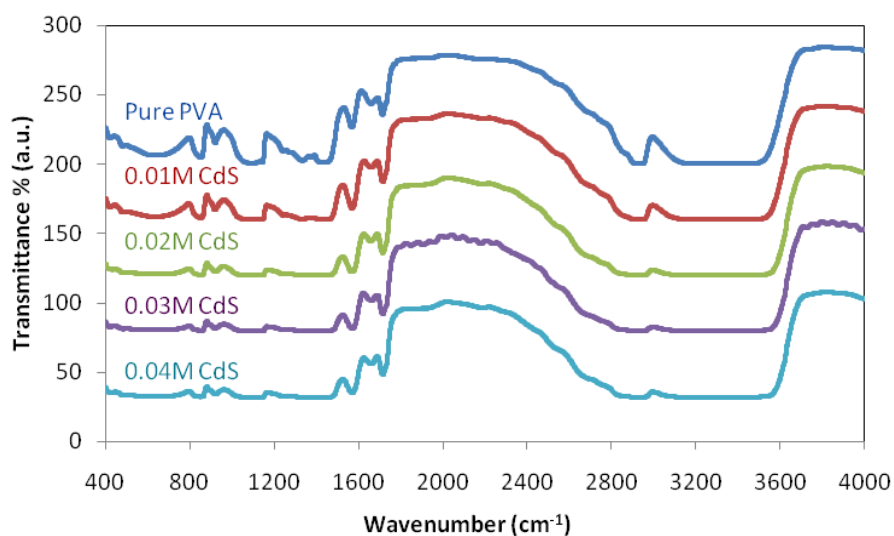


Figure 3. FTIR spectra of pure PVA, and different compositions of PVA/CdS nanocomposite films.

A broad and strong band between 3185 to 3454 cm^{-1} arises from stretching vibration of hydroxyl (-OH) groups [42]. The C-H symmetric and antisymmetric stretching vibrations are observed at 2902 and 2942 cm^{-1} respectively. A Peak at 1713 cm^{-1} is associated with the C=O stretching vibration of PVA backbone. The characteristic infrared peaks at 1659 and 1567 cm^{-1} are corresponding to the C=C terminal and middle double bonds, respectively. A sharp band at 1092 cm^{-1} is responsible for C-O-C stretching of acetyl group present in the PVA backbone.

By comparing the infrared spectrum of pure PVA with that of PVA/CdS samples, it is clear that all spectra mainly exhibit the same features, but the intensity and the position of the peaks were changed. The important result of this study is while increasing the CdS nanocomposite concentration, the peak area of O-H, C=O and C=C are increased, with some shift in their position, this indicates that the coordination between CdS and PVA polymer chains was taken place [43].

3.4 Electrical characterization

The study of the electrical conductivity of polymer nanocomposite gives valuable information about the behaviour of electric charge carriers which leads to good understanding and explanation of conduction mechanism of polymer-based nanocomposites [44].

Fig. 4 illustrates the frequency dependence of ac conductivity σ_{ac} of pure and CdS doped PVA films at room temperature. It can be noted that σ_{ac} increases with frequency especially at high frequencies. This increment in σ_{ac} attributed to the hopping mechanism that occurs under the influence of an externally applied electrical field [45].

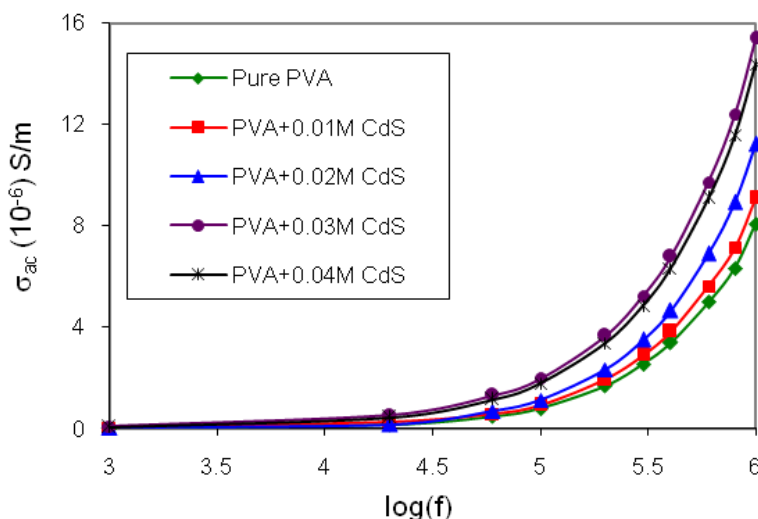


Figure 4. Ac-conductivity as a function of frequency at room temperature for different compositions of PVA/CdS nanocomposite films.

The frequency dependence of the ac conductivity in highly disordered system obeys the Jonscher's universal power law [46,47], expressed as following:

$$\sigma_{ac} = \beta \omega^s \quad (1)$$

where β is frequency-independent, temperature-dependent parameter, ω is the angular frequency and s is frequency exponent, its value is in the interval between 0 and 1 [48]. It has been used to characterize the electrical conduction mechanism in the materials, and the behavior of s value can be explained by several theoretical models.

The variation of ac-conductivity σ_{ac} data with angular frequency has been plotted according to Jonscher’s power law, as shown in Fig. 5. The value of frequency exponent s were obtained from the slopes of $\log(\sigma_{ac})$ versus $\log(\omega)$ for all compositions at different temperatures. The convenient conduction mechanism was determined from the temperature behavior of s .

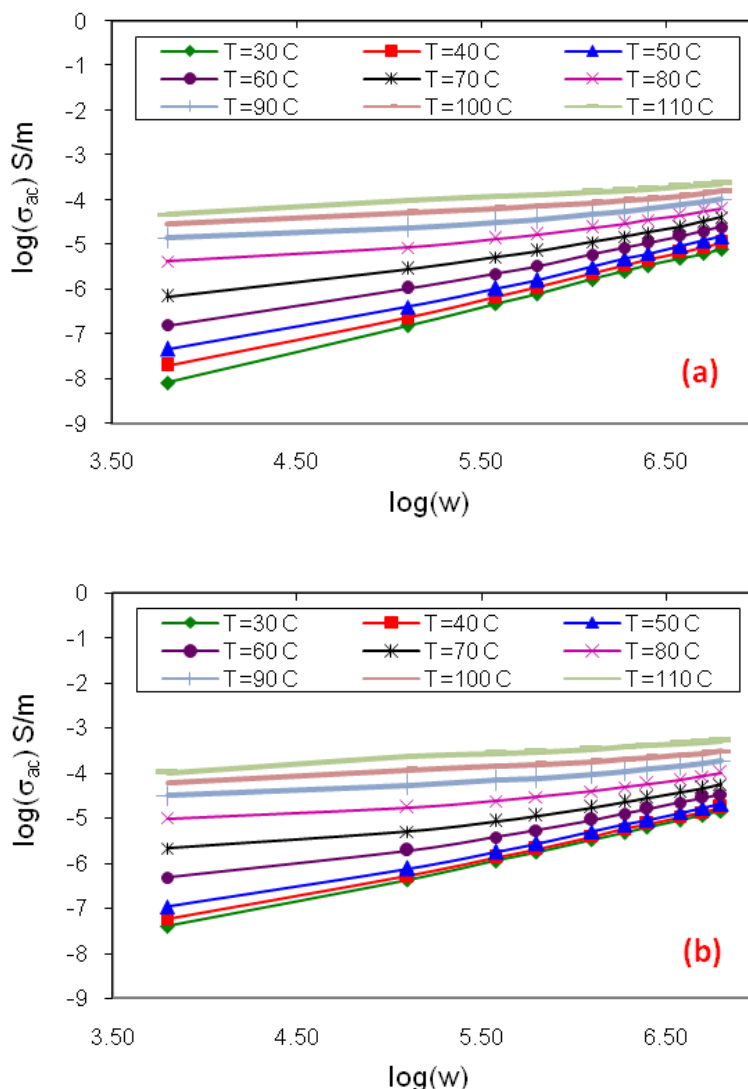


Figure 5. Variation of $\log(\sigma_{ac})$ with $\log(\omega)$ for: (a) Pure PVA, (b) PVA doped 0.04M CdS.

The variation of frequency exponent s as a function of temperature is shown in Fig. 6. It is clearly seen that the values of s approaches its maximum values at low-temperature, and decreased upon increasing temperature.

This behaviour suggests that correlated barrier hopping model (CBH) is applicable to the present nanocomposite samples. In the CBH model that describes charge carrier hops between sites

over the potential barrier separating them, according to this model the value of s decreases with the temperature increment [49].

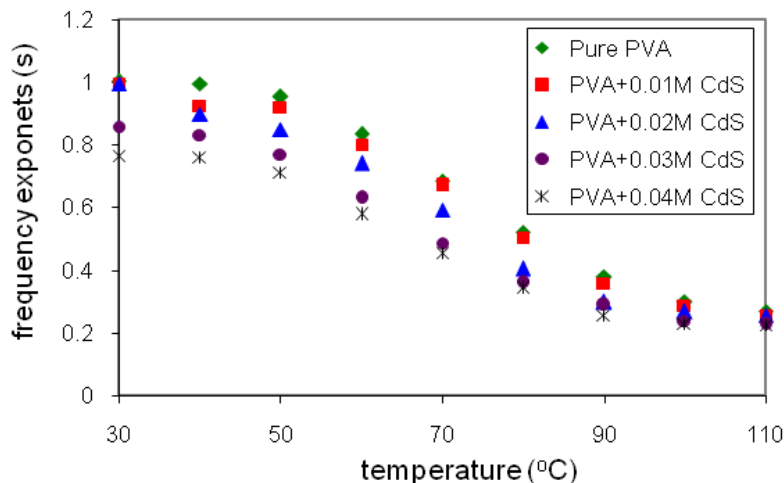


Figure 6. The frequency exponents s versus temperature for pure PVA and different composition of PVA/CdS polymer nanocomposites films.

Also, it can be noted from Fig. 5, that the ac conductivity σ_{ac} increases with increasing temperature in both pure and CdS doped PVA polymer matrix. The dependence of ac conductivity σ_{ac} on temperature is given according to the well-known Arrhenius equation of the form [50]:

$$\sigma_{ac} = \sigma_o \exp\left(-\frac{E_a(\omega)}{K_B T}\right) \quad (2)$$

where σ_o is the pre-exponential factor, $E_a(\omega)$ is the electrical activation energy, K_B is Boltzmann constant and T represents the temperature in Kelvin [51].

The values of ac activation energies E_a at different frequencies were calculated from the slopes of the linear fit of the graph of $\log \sigma_{ac}$ versus $1000/T$ (Arrhenius plots), showing in Fig. 7. The Arrhenius plots indicate the presence of two stages of conductivity, which can be explained by studying the activation behavior of the composites [52].

The first activation energy E_1 occurs at temperature range (60-110 °C) explained by the conduction mechanism due to the conduction of thermal excitation of carriers to the band edges; while the second activation energy E_2 occurs at temperature range (30-60 °C) is due to hopping mechanism between coordinating sites and segmental motion of polymer chains [53].

Begum *et al.* [54] also reported two regions of conduction mechanism for PVA doped Bi_2S_3 nanorods at a temperature range (25-110 °C). A similar behaviour was also shown by Bhargav *et al.* [55] for polymer electrolyte based on PVA doped NaI at a temperature range (30-100 °C). To the best of our knowledge, this is the first report deals the effect of CdS concentration and frequencies of the applied electrical field on the ac activation energy of PVA/CdS polymer nanocomposite.

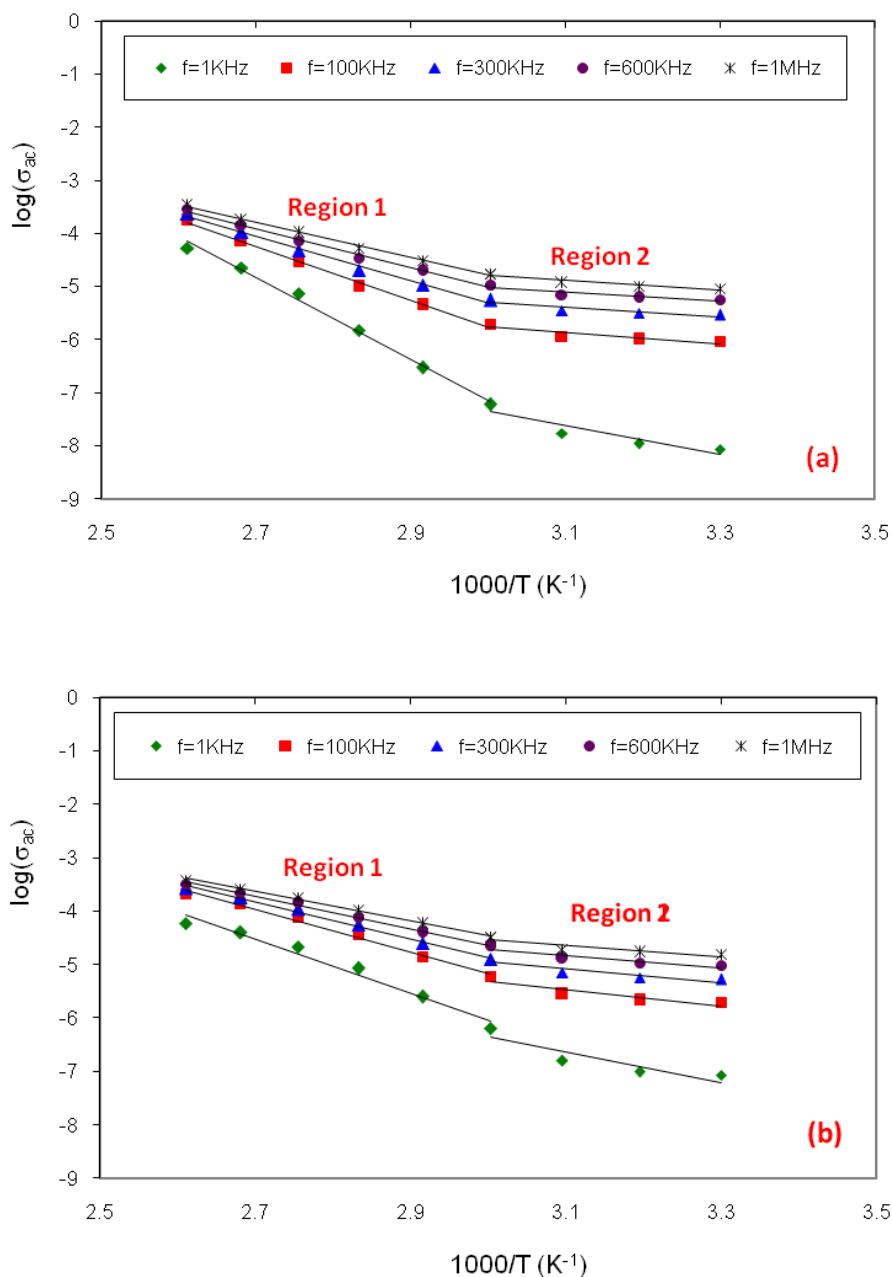


Figure 7. Arrhenius plots of the temperature dependence of σ_{ac} for: (a) pure PVA, and (b) PVA doped 0.04M CdS polymer nanocomposites.

The composition dependence of ac activation energies for the present nanocomposite samples at a different frequency are shown in Fig. 8. It is observed that the activation energies decrease with an increment of the applied electrical field frequency. The increase in frequency enhances the charge carriers to jump between the localized states; consequently, the electrical activation energy decreases with rising frequency [56]. Similar behaviour was shown previously for PVA doped with H_3PO_4 by Prajapati *et al.* [57].

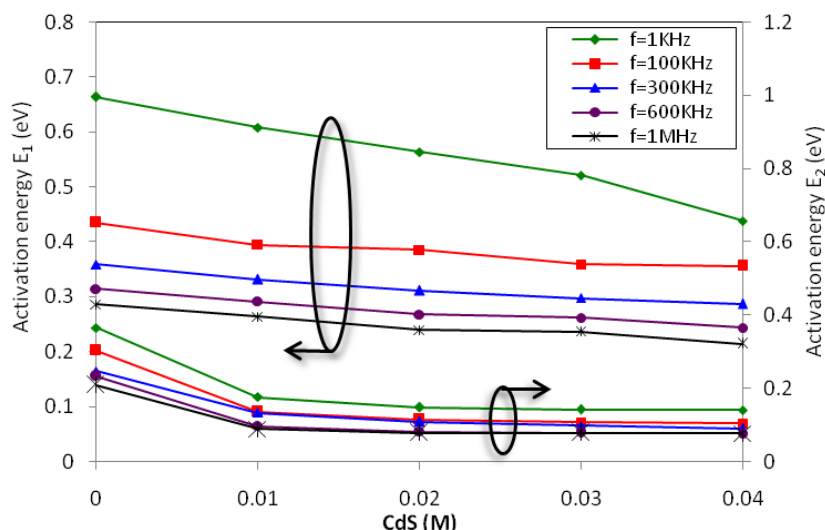


Figure 8. Activation energy versus CdS concentration for PVA/CdS polymer nanocomposite, at different frequency.

Also, it can be noted from Fig. 8, that the value of activation energies decreased with increasing the concentration of CdS nanoparticles in the polymer matrix, which may be related to the reduction of the cross-linking degree of PVA matrix, which confirmed by XRD analysis in Fig. 2. The lower degree of cross-linking severely increases the molecular mobility of polymer chains [58]. The activation energy values obtained for PVA/CdS nanocomposite were smaller than 0.61 eV. Thus, this type of materials could be a suitable candidate for photovoltaic cells [25].

4. CONCLUSIONS

In this work, PVA/CdS polymer based nanocomposite films have been prepared using in-situ chemical reduction, and solution cast techniques. The XRD analysis indicated that the PVA exhibited a typical semi-crystalline structure. The ac conductivity of the present nanocomposite samples shows frequency and temperature dependent. The variation of frequency exponent s versus temperature suggests that correlated barrier hopping model is the most reasonable model to characterize the electrical conduction mechanism of the present system. It was found that the ac activation energy values shifted to lower energies on doping with CdS nanoparticles, and increased with increasing of the applied field frequency. The low activation energy values of PVA/CdS nanocomposite makes it a good candidate for optoelectronic devices.

ACKNOWLEDGEMENT

The Authors desires to thank the University of Sulaimani and University of Human Development, for providing financial support for this research. The authors also gratefully acknowledge the Charmo University, and Kurdistan Institution for Strategic Studies and Scientific Research for the facility in their laboratories.

References

1. D. Paula, and L.M. Robeson, *Polymer* 49 (2008) 3187.
2. P. Nandakumar, C. Vijayan, K. Dhanalakshmi, G. Sundararajan, P.K. Nair, and Y.V.G.S. Murti, *Mater. Sci. Eng.* B83 (2001) 61.
3. S.D. Meenakshi, M. Rajarajan, S. Rajendran, Z.R. Kennedy, and G. Brindha, *Elixir. Nanotechnology* 50 (2012) 10618.
4. K. Ariga, *J. Inorg. Organomet. Polym. Mater.* 25 (2015) 177.
5. K. Ariga, Q. Ji, W. Nakanishi, J.P. Hill, and M. Aono, *Mater. Horiz.* 2 (2015) 406.
6. S. Berciaud, L. Cognet, P. Tamarat, and B. Lounis, *Nano. Lett.* 5 (2005) 515.
7. K.L. Kelly, E. Coronado, L.L. Zhao, and G.C. Schatz, *J. Phys. Chem. B* 107 (2003) 668.
8. S. B. Aziz, O. Gh. Abdullah, D.R. Saber, M.A. Rasheed, and H.M. Ahmed, *Int. J. Electrochem. Sci.* 12 (2017) 363.
9. J. Yao, G. Zhao, D. Wang, and G. Han, *Mater. Lett.* 59 (2005) 3652.
10. A. Kharazmi, E. Saion, N. Faraji, N. Soltani, and A. Dehzangi, *Chin. Phys. Lett.* 30 (2013) 057803.
11. V. Bala, M. Sharma, S.K. Tripathi, and R. Kumar, *Mater. Chem. Phys.* 146 (2014) 523.
12. J. Kakati, and P. Datta, *J. Lumin.* 138 (2013) 25.
13. J. Koteswararao, R. Abhishek, S.V. Satyanarayana, G.M. Madhu, and V. Venkatesham, *eXPRESS Polym. Lett.* 10 (2016) 883.
14. P.K. Ghosh, *Int. J. Hybrid Inf. Technol.* 8 (2015) 49.
15. D. Saikia, P.K. Saikia, P.K. Gogoi, M.R. Das, P. Sengupta, and M.V. Shelke, *Mater. Chem. Phys.* 131 (2011) 223.
16. Y.A. Kalandaragh, *Optoelectron. Advanc. Mater.* 4 (2010) 1655.
17. A. Kharazmi, E. Saion, N. Faraji, R.M. Hussin, and W.M.M. Yunus, *Radiat. Phys. Chem.* 97 (2014) 212.
18. D.C. Onwudiwe, T.P.J. Kruger, O.S. Oluwatobi, and C.A. Strydom, *App. Surf. Sci.* 290 (2014) 18.
19. K.H. Kim, and W.H. Jo, *Composites Sci. Tech.* 68 (2008) 2120.
20. S.F. Bdewi, O.Gh. Abdullah, B.K. Aziz, and A.A.R. Mutar, *J. Inorg. Organomet. Polym. Mater.* 26 (2016) 326.
21. M.H. Makled, E. Sheha, T.S. Shanap, and M.K. El-Mansy, *J. Adv. Res.* 4 (2013) 531.
22. P.M. Buschbaum, *Adv. Mater.* 26 (2014) 7692.
23. R. Kroon, M. Lenes, J.C. Hummelen, P.W.M. Blom, and B.D. Boer, *Polymer Reviews* 48 (2008) 531.
24. C. Kanimozhi, P. Balraju, G.D. Sharma, and S. Patil, *J. Phys. Chem. B* 114 (2010) 3095.
25. E. Sheha, H. Khoder, T.S. Shanap, M.G. El-Shaarawy, and M.K. El-Mansy, *Optik.* 123 (2012) 1161.
26. L.L. Beecroft, and C.K. Ober, *Chem. Mater.* 9 (1997) 1302.
27. R.V. Kumar, R. Elgamiel, Y. Diamant, and A. Gedanken, *Langmuir* 17 (2001) 1406.
28. A. El-Khodary, A.H. Oraby, and A.E. Youssef, *Int. J. Mat. Sci.* 3 (2008) 11.
29. P.K. Khanna, R.R. Gokhale, V.V.V.S. Subbarao, N. Singh, K.W. Jun, and B.K. Das, *Mater. Chem. Phys.* 94 (2005) 454.
30. O.Gh. Abdullah, S.B. Aziz, and M.A. Rasheed, *Results in Physics* 6 (2016) 1103.
31. I.S. Elashmawia, N.A. Hakeema, and M.S. Selim, *Mater. Chem. Phys.* 115 (2009) 132.
32. Y. Wang, A. Suna. W. Mahler, and R. Kasowski, *J. Chem. Phys.* 87 (1987) 7315.
33. K. Pal, U.N. Maiti, T.P. Majumder, P. Dash, N.C. Mishra, N. Bennis, and J.M. Oton, *J. Mol. Liq.* 164 (2011) 233.
34. O. Gh. Abdullah, *J. Zankoy Sulaimani A* 17 (2015) 185.
35. Di Zhang, *Morphology Genetic Materials Templated from Nature Species*, Springer, Verlag Berlin Heidelberg (2012).
36. S. Elliot, *The Physics and Chemistry of Solids*, John Wiley & Sons, New York (1998).

37. O.Gh. Abdullah, and S.A. Saleem, *J. Electron. Mater.* 45 (2016) 5910.
38. K.S. Babu, C. Vijayan, and P. Haridoss, *Mater. Lett.* 60 (2006) 124.
39. O.Gh. Abdullah, *J. Mater. Sci.: Mater. Electron.* 27 (2016) 12106.
40. S. Sarma, and P. Datta, *Nanoscience and Nanotechnology Letters* 2 (2010) 261.
41. R.P. Chahal, S. Mahendia, A.K. Tomar, and S. Kumar, *J. Alloy Compd.* 538 (2012) 212.
42. X. Yuan, *Polym. Bull.* 67 (2011) 1785.
43. S. Gandhi, P. Abiramipriya, N. Pooja, J.J.L. Jeyakumari, A.Y. Arasi, V. Dhanalakshmi, M.R.G. Nair, and R. Anbarasan, *J. Non-Cryst. Solids* 357 (2011) 181.
44. K. Sato, M. Yamaura, T. Hagiwara, K. Murata, and M. Tokumoto, *Synthetic Met.* 40 (1991) 35.
45. O.Gh. Abdullah, Y.A.K. Salman, and S.A. Saleem, *J. Mater. Sci.: Mater. Electron.* 27 (2016) 3591.
46. J. Yang, X.J. Meng, M.R. Shen, L. Fang, J.L. Wang, T. Lin, J.L. Sun, and J.H. Chu, *J. Appl. Phys.* 104 (2008) 104113.
47. S.B. Aziz, and Z.H.Z. Abidin, *Mater. Chem. Phys.* 144 (2014) 280.
48. A.K. Jonscher, *J. Mater. Sci.* 13 (1978) 553.
49. K. Ulutas, D. Deger, and S. Yakut, *J. Phys.: Conference Series* 417 (2013) 012040.
50. N. Reddeppa, A.K. Sharma, V.V.R.N. Rao, and W. Chen, *Measurement* 47 (2014) 33.
51. E. Sheha, and M.K. El-Mansy, *J. Power Sources* 185 (2008) 1509.
52. G. Chakraborty, K. Gupta, D. Rana, and A.K. Meikap, *Adv. Nat. Sci.: Nanosci Nanotechnol* 4 (2013) 025005.
53. C.V.S. Reddy, A.K. Sharma, and V.V.R.N. Rao, *Polymer* 47 (2006) 1318.
54. A. Begum, A. Hussain, and A. Rahman, *Mater. Sci. Appl.* 2 (2011) 163.
55. P.B. Bhargav, V.M. Mohan, A.K. Sharma, and V.V.R.N. Rao, *Int. J. Polym. Mater.* 56 (2007) 579.
56. P. Kalugasalam, and S. Ganesan, *Chalcogenide. Lett.* 6 (2009) 469.
57. G.K. Prajapati, and P.N. Gupta, *Nucl. Instrum. Methods in Phys. Res. B* 267 (2009) 3328.
58. T. Kaiser, *Prog. Polym. Sci.* 14 (1989) 373.